

Electric Field Effect on Polarized Photon Emission of Foil Excited Hydrogen Atoms

By

Yasuyuki Kimura* and Keishi Ishii*

(Received October 13, 1993)

Abstract

We have calculated the beam current density effect on the degree of polarization of the Balmer α line emission from the foil-excited hydrogen atoms, by the model of a static electric field at the exit surface of the carbon foil. The results agree with the experiments. The disagreements still left are discussed.

1 Introduction

In the present paper, we report a calculation of the beam current density effect on the degree of polarization of the Balmer α line emission from the foil-excited hydrogen atoms. In the beam foil experiment, light emitted from fast atoms excited upon passage through a thin carbon foil is observed in the downstream of the foil. Berry *et al.* reported that the degree of polarization of He I lines are dependent on the foil tilt angle with respect to the beam velocity.¹⁾ Further experiments have confirmed the tilt angle dependence for a variety of atoms and ions.²⁻⁵⁾ Eck has presented the first theoretical study of the production of anisotropy of excited states upon passage through a tilted foil using a model.⁶⁾ He assumed the existence of the strong electric field along the foil normal in the vicinity of the foil, and the field strength is of the order of 10^8 V/cm within a few Bohr radii and falls off rapidly. The theoretical studies have been further extended.⁷⁻¹⁰⁾

In addition to the dependence of the polarization on the foil tilt angle, a substantial dependence on the beam current density was observed for helium atoms¹¹⁻¹⁴⁾ and for hydrogen atoms.^{8, 9, 18)} This is also attributed to the strong electric field near the rear surface of the foil resulting from the secondary electron emission caused by a penetration of the ion beams. The magnitude of the field strength estimated is different among authors. Gay and Berry¹²⁾ reported $\sim 10^8$ V/cm over 10 \AA , while Weber *et al.*¹⁰⁾ showed 6.2×10^5 V/cm.

* Department of Engineering Science

Both works are on helium atoms. There is no significant difference in the secondary emission yield of electrons from thin carbon foils for different projectile ion species.¹⁵⁾ The field of $\sim 10^8$ V/cm is high enough to field-ionize $n=3$ and higher lying levels of hydrogen atoms. In such a high field, no lines of Balmer series are formed.

The present calculation clarified the relation between the degree of polarization and the existing electric field strength, based on the assumption of a static electric field model. When applied to the hydrogen Balmer α emission, it was shown that the degree of polarization begins to increase at ~ 10 V/cm and its appreciable change is detectable at a field strength of the order of 10 V/cm. Details are shown in the following sections.

2 Time Evolution of Density Matrix in Electric Field

The essential parts of the model in the present work are the following assumptions : i) The electrostatic forces are important in the beam-foil interaction : the interaction acts only on the orbital angular momentum and leaves the spin isotropic.¹⁷⁾ ii) The foil normal is parallel to the beam velocity direction, thereby excitation process has a reflection and an axial symmetry. iii) The initial excited states are formed exactly on the rear surface of the foil (at time $t=0$). iv) The excited states are perturbed by the electric field in the vicinity of the rear surface for a time duration T . The field is produced by the uniformly distributed charge on the foil surface, and its direction is parallel to the beam. Furthermore, the individual atom experiences the same field over the beam diameter. v) Hyperfine structure was not included in the present study.

The state of n -th hydrogen atom at $t=0$ is described as¹⁶⁾

$$|\Psi^{(n)}(0)\rangle = \sum_{lm, m_s} a_{lm, m_s}^{(n)} |lm\rangle |sm_s\rangle. \quad (1)$$

The density matrix operator $\rho(0)$ is represented as

$$\begin{aligned} \rho(0) &= \frac{1}{N} \sum_n |\Psi^{(n)}(0)\rangle \langle \Psi^{(n)}(0)| \\ &= \frac{1}{N} \sum_n \sum_{lm, m_s} \sum_{l' m'_s} a_{lm, m_s}^{(n)} a_{l' m'_s}^{(n)*} |lm\rangle |sm_s\rangle \langle sm'_s| \langle l' m'_s| \\ &= \sum_{lm, m_s} \sum_{l' m'_s} \rho_{ll' m'_s m_s}^{unc} |lm\rangle |sm_s\rangle \langle sm'_s| \langle l' m'_s|, \end{aligned} \quad (2)$$

where N is the total number of the hydrogen atoms in this ensemble and $\rho_{ll' m'_s m_s}^{unc}$ is a density matrix element in the uncoupled basis set,

$$\rho_{ll' m'_s m_s}^{unc} = \frac{1}{N} \sum_n a_{lm, m_s}^{(n)} a_{l' m'_s}^{(n)*} = \langle a_{lm, m_s} a_{l' m'_s}^* \rangle,$$

where $\langle \dots \rangle$ stands for the ensemble average.

By taking into account the interaction nature (assumption i)) and the geometrical sym-

metry (assumption ii)), the density matrix element can be simplified as

$$\rho_{ll' m_l m_l' m_s m_s'}^{unc} = \rho_{ll' m_l m_l' m_s m_s'}^{unc} \delta_{m_l m_l'} \delta_{m_s m_s'}.$$

Another condition derived from the assumption i) is such that ρ is irrelevant of sign of m_l . Then the density matrix element can be written as $\rho_{ll' |m_l|}^{unc}$. Therefore, Eq. (2) is finally represented by,

$$\rho(0) = \sum_{ll' m_l m_l'} \rho_{ll' |m_l|}^{unc} |lm\rangle |sm\rangle \langle sm| \langle l' m_l| \quad (3)$$

The explicit form of the matrix element in the uncoupled basis is also written as,

$$\langle l' m_l' m_s' | \rho(0) | lm \rangle = \rho_{ll' |m_l|}^{unc} \delta_{m_l m_l'} \delta_{m_s m_s'}. \quad (4)$$

The uncoupled basis representation is suitable for describing the state just after the excitation, *i. e.* $t=0$. For $t>0$, the state can be described in the coupled basis set $\{|(l, s) j, m\rangle\}$. The conversion from the uncoupled representation to the coupled one is given by

$$|(ls)jm\rangle = (-1)^{s-l-m_j} \sum_{m_l m_s} \sqrt{2j+1} \begin{pmatrix} l & 1/2 & j \\ m_l & m_s & -m_j \end{pmatrix} |lm\rangle |sm\rangle. \quad (5)$$

The time evolution of the density matrix $\rho(t)$ is given by

$$\rho(t) = U(t)\rho(0)U(t)^\dagger. \quad (6)$$

The time evolution operator $U(t)$ satisfies following relation :

$$i\hbar \frac{\partial U(t)}{\partial t} = H(t) U(t). \quad (7)$$

The Hamiltonian $H(t)$ is given as a sum of three parts as follows :

$$H(t) = H_0 + H_D + H_F(t). \quad (8)$$

Here H_0 is the free atom Hamiltonian and H_D describes the decay. They satisfy the following pair of equations :

$$H_0 |(ls)jm\rangle = E_y |(ls)jm\rangle = \hbar\omega_y |(ls)jm\rangle, \quad (9)$$

$$H_D |(ls)jm\rangle = -\frac{i}{2}\hbar\Gamma_l |(ls)jm\rangle, \quad (10)$$

where $E_y (= \hbar\omega_y)$ and Γ_l are the energy eigenvalue and the decay constant of the state $|(ls)jm\rangle$, respectively. The Stark Hamiltonian $H_F(t)$ is time dependent due to the static electric field $F(t)$ for the fast moving hydrogen atom, and is given by,

$$H_F(t) = -\mathbf{d} \cdot \mathbf{F}(t) = -(-e)\mathbf{r} \cdot \mathbf{F}(t),$$

where \mathbf{d} is the electric dipole moment and $-e$ is the electron charge ($e > 0$).

In the geometry assumed here, the beam axis is chosen in the $+z$ direction and chosen as the quantization axis. The electric field is then $+z$ direction, too. The field $\mathbf{F}(t)$ can be written as $F_z(t)$, where $F_z(t)$ denotes the z component of the field $\mathbf{F}(t)$. Therefore, the Stark Hamiltonian is given as

$$H_F(t) = +e z F_z(t). \quad (11)$$

The matrix element of $H_F(t)$ is described in the coupled basis as,

$$\begin{aligned} & \left\langle \left(l' \frac{1}{2} \right) j' m'_j \middle| H_F(t) \middle| \left(l \frac{1}{2} \right) j m_j \right\rangle \\ &= (-1)^{j+j'-m'_j+3/2} e F_z(t) \sqrt{2l+1} \sqrt{2l'+1} \sqrt{2j+1} \sqrt{2j'+1} \\ & \quad \begin{pmatrix} j' & 1 & j \\ -m'_j & 0 & m_j \end{pmatrix} \begin{pmatrix} l' & 1 & l \\ 0 & 0 & 0 \end{pmatrix} \begin{Bmatrix} l' & j' & 1/2 \\ j & l & 1 \end{Bmatrix} \langle n l' | r | n l \rangle. \end{aligned} \quad (12)$$

Since the elapsed time in the field for an atom moving with the velocity v is given by $t = z/v$, the field $F_z(t)$ can also be represented as a function of z by $F_z(z)$. Assuming iv), the field distribution produced by a positively charged foil with areal charge density σ is given as

$$\begin{aligned} F_z(z) &= \frac{\sigma}{2\epsilon_0} \left(1 - \frac{z}{\sqrt{a^2 + z^2}} \right) \\ &= F_0 \left(1 - \frac{z}{\sqrt{a^2 + z^2}} \right), \end{aligned} \quad (13)$$

where ϵ_0 is the permittivity in vacuum and a is the radius of the foil. Therefore, the field $F_z(t)$ is given by

$$F_z(t) = F_0 \left(1 - \frac{vt}{\sqrt{a^2 + (vt)^2}} \right). \quad (14)$$

The density matrix $\rho(T)$ at time $t = T$ perturbed by the field $F_z(t)$ is then estimated by using Eq. (6) through Eq. (14). The differential equation Eq. (7) has been solved numerically by using the Runge–Kutta–Gill method.

3 Results and Discussions

With the method described in the previous section, we have calculated the density matrix $\rho(T)$ starting from a set of initial density matrix elements of $\rho(0)$ listed in Table 1. They are deduced from our intensity decay measurement of the Balmer α line using the beam foil technique.¹⁸⁾ Here the alignments in p- and d-states are assumed to be zero. The

Table 1. Initial density matrix elements on uncoupled basis used in the present calculation.

Density matrix element	Adopted value real	imag
σ_{ss0}	0.50	
σ_{pp0}	0.10	
σ_{pp1}	0.10	
σ_{dd0}	0.04	
σ_{dd1}	0.04	
σ_{dd2}	0.04	
σ_{sd0}	0.01	0.01
σ_{pd0}	0.00	0.00
σ_{pd1}	0.00	0.00
σ_{sp0}	0.00	0.00

assumption makes it possible to see clearly the onset and the time development of the alignment by the perturbation in the field $F(t)$. The initial density matrix is normalized to unity. Only one coherence term σ_{sd0} among four possible terms is included.

The density matrix $\rho(T)$ thus calculated was used to estimate the alignment parameter A_0^{col} introduced by Fano and Macek¹⁷⁾ to characterize the polarization of the states,

$$A_0^{col}(p) = \frac{-\sigma_{pp0} + \sigma_{pp1}}{\sigma_{pp0} + 2\sigma_{pp1}}, \quad (15)$$

$$A_0^{col}(d) = \frac{-\sigma_{dd0} - \sigma_{dd1} + 2\sigma_{dd2}}{\sigma_{dd0} + 2\sigma_{dd1} + 2\sigma_{dd2}}. \quad (16)$$

The calculated alignment parameter for p- and d-states is plotted against the field strength F_0 on the rear surface of the foil, and is shown in Fig. 1. The values of A_0^{col} are for those at $z=20$ mm in the downstream of the foil, where the field strength is less than 1% of F_0 .

The results show that the A_0^{col} for both p- and d-states stays zero for the field below 10 V/cm and grows gradually on the negative side with the field F_0 . The negative sign of $A_0^{col}(p)$ and $A_0^{col}(d)$ means that as the field F_0 goes higher, that is, as the beam current density increases, the p and d electrons of the foil-excited hydrogen atoms are more populated along the beam axis than in the direction perpendicular to the beam. In other words, the degree of polarization of the emitted photon intensity increases as the incident beam current density increases. This qualitative tendency is in agreement with the experiments on He I¹⁴⁾, and on hydrogen Balmer β line⁸⁾.

An important point to be discussed here is the relation between the beam current den-

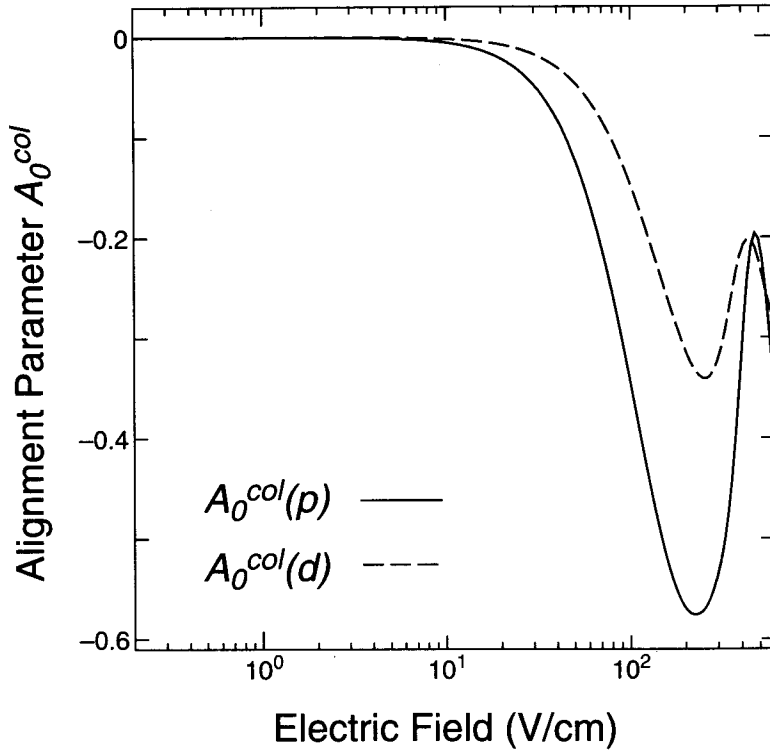


Fig. 1. — Alignment parameter $A_0^{col}(p)$ for 3p level of hydrogen atom and ---- $A_0^{col}(d)$ for 3d level as a function of static electric field strength F_0 .

sity and the field strength F_0 on the rear surface of the foil. It seems natural that the field F_0 increases with the beam current⁹⁾ or beam current density¹⁴⁾, as far as its main reason is assumed to be due to the secondary electron emission by the beam penetration. Since the close relationship between them is not yet clear, we have calculated A_0^{col} as the function of F_0 .

From Fig. 1, it is seen that after reaching a minimum at the field of about $\sim 2 \times 10^2$ V/cm, the alignment goes back, and starts to oscillate. This oscillation is caused by the Stark quantum beats. In the electric dipole approximation, the emitted photon intensity for the transition from the state $|\Psi(t)\rangle$ to a group of lower state $|0\rangle$ is given by

$$I^P(t) = K \sum_0 |\langle 0 | X^P | \Psi(t) \rangle|^2, \quad (17)$$

where K is a constant of proportionality and X^P is the electric dipole operator with the polarization P . The upper state $|\Psi(t)\rangle$ is estimated by solving the Schrödinger equation :

$$H(t) | \Psi(t) \rangle = \hbar \omega(F) | \Psi(t) \rangle$$

The Eq. (17) is then written in the following form as a function of time t and field F :

$$I^P(F, t) = I_0 \sum_i \exp[-\Gamma_i(F)t] [A_i^P(F) + B_i^P(F) \cos \omega_i(F)t], \quad (18)$$

where I_0 is the detection efficiency, and $A_i^P(F)$ and $B_i^P(F)$ are dependent on the field F , polarization P and the transition probability of the upper level, and $\omega_i(F)$ is the frequency between the levels in the field.

The second term in Eq. (18) gives the modulation superposed on the constant term $A_i^P(F)$ with the decay $\Gamma_i(F)$. The quantum beat is usually observed along the beam path by the time differential way in the beam foil spectroscopy. However, as is seen in Eq. (18), another type of modulation can also be obtained as the function of field F when observed at a fixed time t , *i. e.* at the fixed position. This second type of modulation in the intensity measurement is called the field differential quantum beat. These are the direct consequences from the Eq. (18). From the physical point of view, the quantum beat is the embodiment of the coherent transfer among the excited levels in the electric field.

The present calculation shows that the polarization of light emitted by a foil excited atom increases with the field strength, when observed from a fixed position after the excitation at the foil. Although this simple model seems physically plausible, and successfully explains the characteristics of the polarization as a function of the incident beam current density, it fails at the highest current density limit. In all the experiments,^{8, 9, 11-14, 18)} the polarization increases monotonously with the current density.

In the experiment, the hydrogen atom in the beam after passage through a foil has a velocity spread to some extent, which is dependent on the incident beam energy and the thickness of the foil, *e. g.* a few % for a 100 keV beam and a $5\mu\text{g}/\text{cm}^2$ thickness foil. This plays an essential role especially in the case where the current density is high. The high frequency beats are smeared out in the time differential measurement, and the oscillation damps in the field differential observation. Therefore, the data obtained in the experiment is the average in time in either experiment. In addition to the above discussion, the foil-life is short because of the damage in the high current density measurement and it is difficult to keep the current density constant throughout measurement. This lowers the quality of the data, in general.

In the present calculation we have assumed a uniform distribution of the charge on the foil surface over the whole area, and a uniform electric field in the downstream of the foil. In the experiment, the distribution of the charge is not uniform because of the finite size and finite electric conductivity of the carbon foil. The electric field induced by the charge is also disturbed partly by the finite size of the foil itself and the foil folder made of metal. The field acting on an atom is different according to the position in the beam of the finite

size of diameter.

We have developed a method to calculate the effect of the static electric field on the degree of polarization of emitted light from a foil excited atom on the assumption of the charge distribution on the rear surface of the foil. The result is shown when applied to the hydrogen Balmer- α transition. A similar calculation can be applied to other transitions, even to other atoms. In this case, the absolute value of the alignment parameter, the degree of polarization are different, and also the absolute scale of the field is different.

The present calculation shows the nonlinear behavior of the increase of the degree of polarization of the emitted light of the foil excited atoms based on the static electric field model.

References

- 1) H. G. Berry, L. J. Curtis, D. G. Ellis and R. M. Schectman ; Phys. Rev. Lett. **32**, 751 (1974).
- 2) G. J. Pedrazzini, R. B. Gardiner and C. H. Liu ; Phys. Lett. **63A**, 23 (1977).
- 3) H. G. Berry, S. N. Bhardwaj, L. J. Curtis and R. M. Schectman ; Phys. Lett. **50A**, 59 (1974).
- 4) H. G. Berry, G. Gablielse and A. E. Livingston ; Phys. Rev. **A16**, 1915 (1977).
- 5) S. Huldt, L. J. Curtis, B. Denne, L. Engström, K. Ishii and I. Martinsin ; Phys. Lett. **66A**, 103 (1978).
- 6) T. G. Eck ; Phys. Rev. Lett. **33**, 1055 (1974).
- 7) Y. B. Band ; Phys. Rev. Lett. **35**, 1272 (1975).
- 8) W. Singer, J. C. Dehaes and J. Carmeliet ; Phys. Scripta **21**, 165 (1980).
- 9) J. C. Dehaes, J. Carmeliet and H. G. Berry ; Phys. Rev. **A40**, 5583 (1989).
- 10) J. P. Weber, J. C. Dehaes and J. Devooght ; Phys. Rev. **A45**, 307 (1992).
- 11) R. D. Hight, R. M. Schectman, H. G. Berry, G. Gablielse and T. Gay ; Phys. Rev. **A16**, 1805 (1977).
- 12) T. J. Gay and H. G. Berry ; Phys. Rev. **A19**, 952 (1979).
- 13) T. J. Gay, H. G. Berry, R. DeSerio, H. P. Garnir, R. M. Schectman, N. Schaffel, R. D. Hight and D. J. Burnus ; Phys. Rev. **A23**, 1745 (1981).
- 14) H. Winter ; Nucl. Instrum. Methods. **194**, 357 (1982).
- 15) J. W. Keller, K. W. Oglivie, J. W. Boring and R. W. McKemie ; Nucl. Instrum. Methods **B61**, 291 (1991).
- 16) M. J. Alguard and C. W. Drake ; Phys. Rev. **A8**, 27 (1973).
- 17) U. Fano and J. Macek ; Rev. Mod. Phys. **45**, 553 (1973).
- 18) Y. Kimura ; unpublished (1992).